Phonon-assisted diffusion in bcc phase of titanium and zirconium from first principles

Sara Kadkhodaei * and Ali Davariashtiyani

Department of Civil and Materials Engineering, University of Illinois at Chicago, Chicago, Illinois 60607, USA



(Received 13 October 2019; revised manuscript received 11 January 2020; accepted 17 March 2020; published 13 April 2020)

Diffusion is the underlying mechanism for many complicated materials phenomena, and understanding it is basic to the discovery of novel materials with desired physical and mechanical properties. Certain groups of solid phases, such as the bcc phase of IIIB and IVB metals and their alloys, which are only stable when they reach high enough temperatures and experience anharmonic vibration entropic effects, exhibit "anomalously fast diffusion." However, the underlying reason for the observed extraordinary fast diffusion is poorly understood and due to the existence of harmonic vibration instabilities in these phases the standard models fail to predict their diffusivity. Here, we indicate that the anharmonic phonon-phonon coupling effects can accurately describe the anomalously large macroscopic diffusion coefficients in the bcc phase of IVB metals and therefore yield understanding on the underlying mechanism for diffusion in these phases. We utilize temperature-dependent phonon analysis by combining *ab initio* molecular dynamics with lattice dynamics calculations to provide an approach to use the transition state theory beyond the harmonic approximation. We validate the diffusivity predictions for the bcc phase of titanium and zirconium with available experimental measurements, while we show that predictions based on harmonic transition state theory severely underestimate diffusivity in these phases.

DOI: 10.1103/PhysRevMaterials.4.043802

I. INTRODUCTION

Diffusion processes play a key role in the kinetics of many materials-related phenomena, such as microstructural evolution during materials processing, and discovery of materials with specific diffusion characteristics is a major effort in various research communities. Understanding mechanisms of diffusion and providing an a priori predictive ability for diffusivity are essential for discovery of materials with specific diffusion characteristics and first-principles methods have become a common approach to predict diffusivity in various materials [1–15]. Existing computational frameworks based on the harmonic transition state theory [16,17] rely on the assumption that the solid phase is metastable and there exists no mechanical instabilities in the system. This assumption impedes the use of standard models to predict diffusivity in many solid-state systems [18–29], including the β phase of group IIIB and IVB metals and their alloys, where the system exhibits harmonic phonon instabilities yet is stabilized at high enough temperatures due to strongly anharmonic lattice vibration entropic effects. Moreover, β phase of IIIB and IVB metals and their alloys exhibit "anomalously fast diffusion," several orders of magnitude higher than fcc metals and other bcc metals, at temperatures far below their melting point [30–36], yet the underlying reason for this anomaly is poorly understood.

A number of studies have proposed explanations for the anomalous fast diffusion in the bcc phase of IIIB and IVB metals [37–45]. While some earlier studies proposed mixed vacancy mechanisms similar to the contribution of divacancies jump or mobile defects in fcc metals as the basis of anomalous fast diffusion, later experimental evidence based on isotope effect measurements and neutron scattering in β IIIB and IVB metals confirmed that the monovacancy mechanism is the predominant diffusion mechanism [31-33,35,46,47]. Recently, Sangiovanni et al. [44] proposed a highly concerted stringlike atomic motion as the mechanism underlying anomalously large self-diffusivities in bcc Ti based on observations in an ab initio molecular dynamics simulation. Other studies correlated the markedly fast diffusion to temperature-induced effects. For example, Sanchez and de Fontaine proposed a model which correlates diffusivity in β -Zr to the formation of the metastable ω phase (i.e., heterophase fluctuations between bcc and ω induced by anharmonic vibrations), in which the diffusion activation energy is assumed to be the formation free energy of the ω embryo [38,39]. Herzig and co-workers concluded that the observed anomalous fast self-diffusion corresponds to the softening of the LA $\frac{2}{3}\langle 111\rangle$ phonon mode [40–42], supported by observation of higher diffusivity in phases with stronger softening effects [40].

The contribution of this report is twofold; First we illustrate that while the monovacancy jump is the predominant mechanism for diffusion in the bcc phase of Ti and Zr, it is promoted by the anharmonic phonon-phonon coupling effects, which underlies the observed anomalously fast diffusion. Second, we provide an approach based on first-principles calculations that can successfully predict the macroscopic diffusion coefficient for the bcc phase of titanium and zirconium where the standard computational frameworks based on harmonic transition state theory fail. We have previously shown that for bcc IVB metals and their compounds (which are mechanically

^{*}Author to whom correspondence should be addressed: sarakad@uic.edu

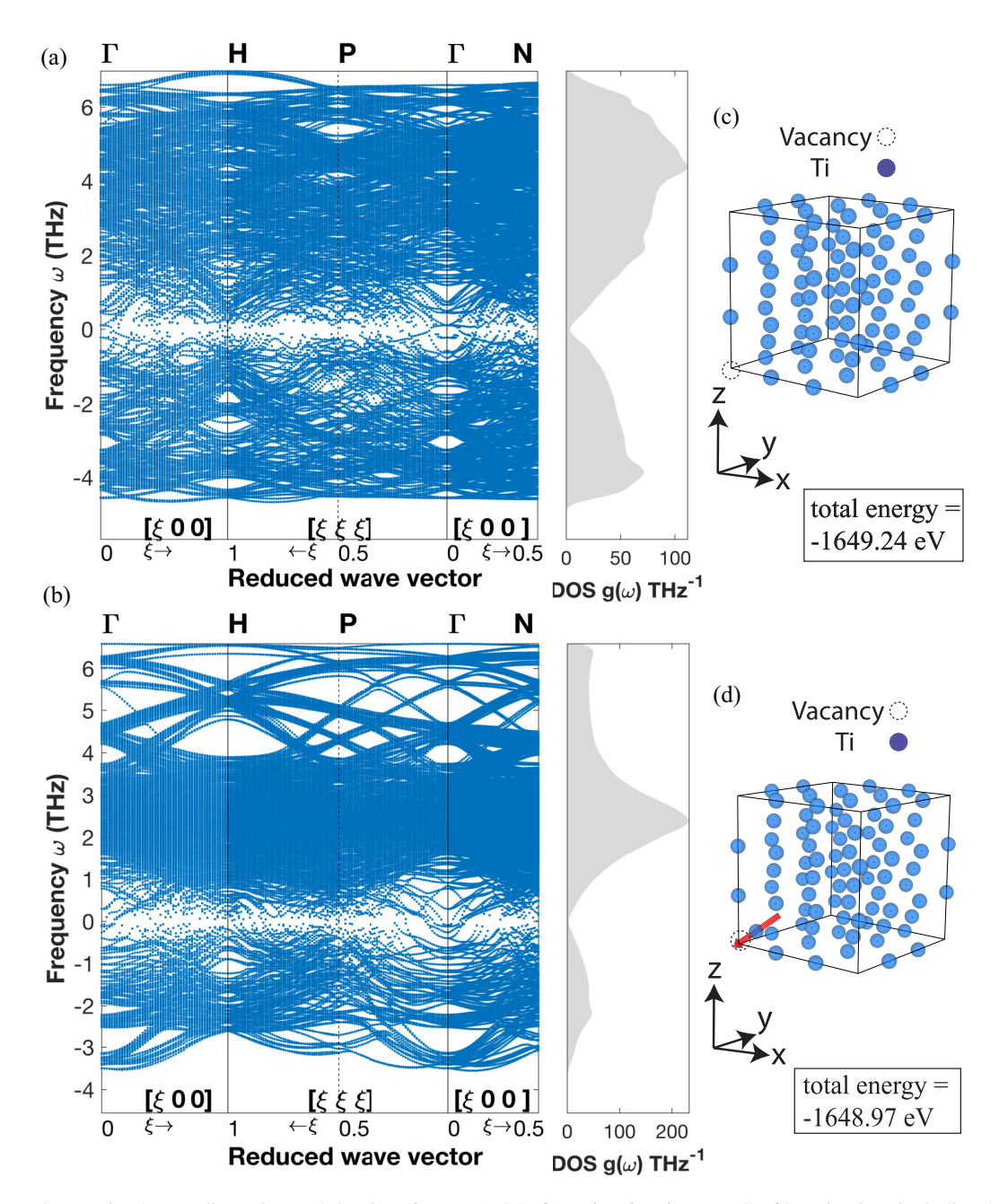


FIG. 1. DFT harmonic phonon dispersion and density of states (DOS) for a $6 \times 6 \times 6$ supercell of bcc titanium including 215 atoms and a monovacancy (a) at the bcc site and (b) migrated halfway to the nearest neighbor bcc site along the [111] direction. Phonon instabilities are depicted as negative frequencies in the dispersion curves. The atomic configuration for the initial and intermediate states of vacancy diffusion are illustrated in (c) and (d), respectively. A conventional supercell is presented for visualization simplicity.

unstable), temperature-induced dynamical stabilization results in hopping of the system among local distortions of the lattice (i.e., local minima) in a way that the average atomic positions stay at bcc [22,28]. These local minima are located along the trigonal path associated with the longitudinal $L_3^2\langle 111\rangle$ phonon eigenvector [22,28]. Here we show that the coincidence of this dynamical hopping with the direction of vacancy jump along $\frac{1}{2}\langle 111\rangle$ nearest neighbor in bcc metals significantly promotes the macroscopic diffusivity. Our a priori prediction is validated with available experimental diffusivity measurements. On the other hand, we indicate that predicting diffusivity based on harmonic lattice vibrations

severely underpredicts this diffusivity. This further illustrates the significant role of anharmonic lattice vibration interactions in enhancing the diffusivity. Our findings shed light on understanding the fundamental origins of diffusion mechanism in entropy-stabilized phases.

II. ANHARMONIC LATTICE VIBRATION EFFECTS WITHIN TRANSITION STATE THEORY

The macroscopic diffusivity D for a vacancy-mediated diffusion can be described in terms of the atomic jump distance

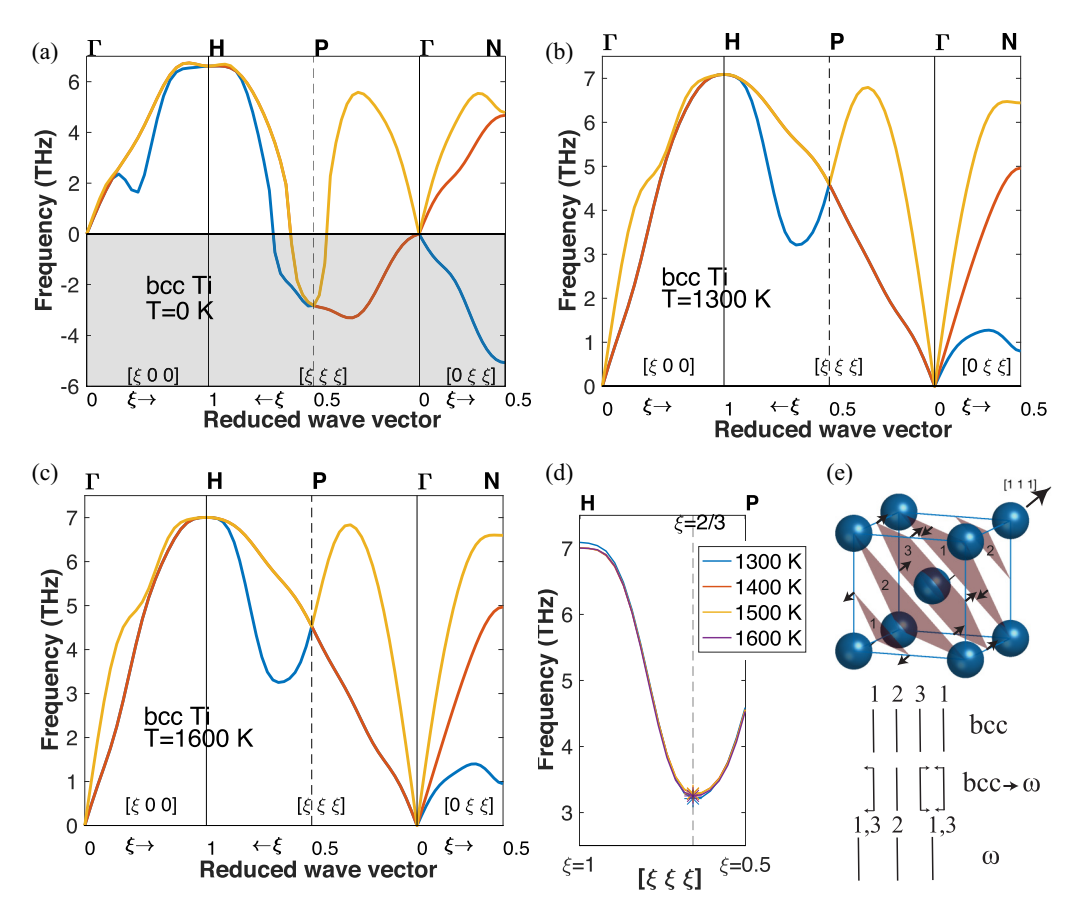


FIG. 2. Phonon dispersion for a bulk defect-free $6 \times 6 \times 6$ supercell of bcc titanium including 216 atoms at (a) 0 K, (b) 1300 K, and (c) 1600 K obtained using the SCAILD method. (d) The longitudinal phonon branch along the $[\xi \xi \xi]$ reduced wave vector (between H and P high-symmetry points) from 1300 K to 1600 K. The star marks in (d) represent the negative dip on the phonon branch. (e) The trigonal distortion of (111) atomic planes along the [111] direction associates with the eigenvector of $\xi = \frac{2}{3}$ phonon mode along the Γ -P-H branch. A complete collapse of atomic planes 1 and 3 results in the hexagonal ω phase.

and jump frequency [48,49] as the following,

$$D = \alpha C_v a^2 \Gamma, \tag{1}$$

where α is a geometrical factor ($\alpha = 8/6$ for bcc), a is the vacancy jump distance, C_v is the equilibrium vacancy concentration, and Γ is the successful vacancy jump frequency [48]. Within the transition state theory [1,16,17,50], the defect jump frequency is expressed as $\Gamma = \nu^* \exp(-\Delta H_m/k_B T)$, where ΔH_m is the migration enthalpy. k_B is the Boltzmann's constant and T denotes temperature. v^* is the effective prefactor frequency, which encompasses all vibrational effects in the diffusion process. Within the harmonic transition state theory (HTST), ν^* is expressed as the ratio of the product of normal vibration frequencies (i.e., harmonic phonon frequencies) of the initial state to that of the nonimaginary normal frequencies of the transition state, $v^* =$ $\frac{\prod_{i=1}^{3N} \nu_i}{\prod_{i=1}^{3N-1} \nu_i'}$, where ν and ν' are the frequencies for the initial and transition configurations, respectively, for a system of N atoms. The equilibrium monovacancy concentration C_v is calculated according to $C_v = \exp(-\frac{\Delta H_v - T \Delta S_v}{k_B T})$, where ΔH_v and ΔS_v are enthalpy and entropy of monovacancy formation, respectively. The formation enthalpy and entropy are calculated according to $\Delta H_v = H^{\rm tot}(N-1) - \frac{N-1}{N} H^{\rm tot}(N)$ and $\Delta S_v = S^{\text{tot}}(N-1) - \frac{N-1}{N}S^{\text{tot}}(N)$, respectively. $H^{\text{tot}}(N-1)$

and $S^{\text{tot}}(N-1)$ are the total enthalpy and entropy for a system with a monovacancy and $H^{\text{tot}}(N)$ and $S^{\text{tot}}(N)$ are the total enthalpy and entropy for the bulk phase, respectively. The vibration entropy for each system is obtained from $S_{\text{vib}} = -k_B \int_0^\infty \ln{[2 \sinh(\frac{\hbar\omega}{2k_B T})]} g(\omega) d\omega$, where ω is the vibration frequency and $g(\omega)$ is phonon density of state (DOS).

For systems that exhibit harmonic phonon instabilities, such as the bcc phase of IVB metals, calculation of diffusivity according to harmonic phonon analysis becomes infeasible. More specifically, the existence of multiple imaginary ν and ν' frequencies impedes the use of HTST to obtain ν^* , and S_{vib} cannot be obtained based on imaginary phonon frequencies. In Fig. 1, the harmonic phonon dispersions for bcc Ti with a monovacancy at the initial and an intermediate state are obtained based on the density-functional theory (DFT) finite displacement approach, where the harmonic phonon dispersions exhibit phonon instabilities (a similar plot for bcc Zr is presented in Fig. S5 in Ref. [51]). However, similar to other bcc IIIB and IVB metals, bcc Ti is stabilized at high enough temperature due to the entropic stabilization of the system arising from large amplitude anharmonic hopping among local distortions [18-22,24,26-28,52-59]. We utilize two different variations of the self-consistent harmonic approximation (SCHA) approach, namely the self-consistent ab initio lattice dynamics (SCAILD) [60–62] and the temperature dependent

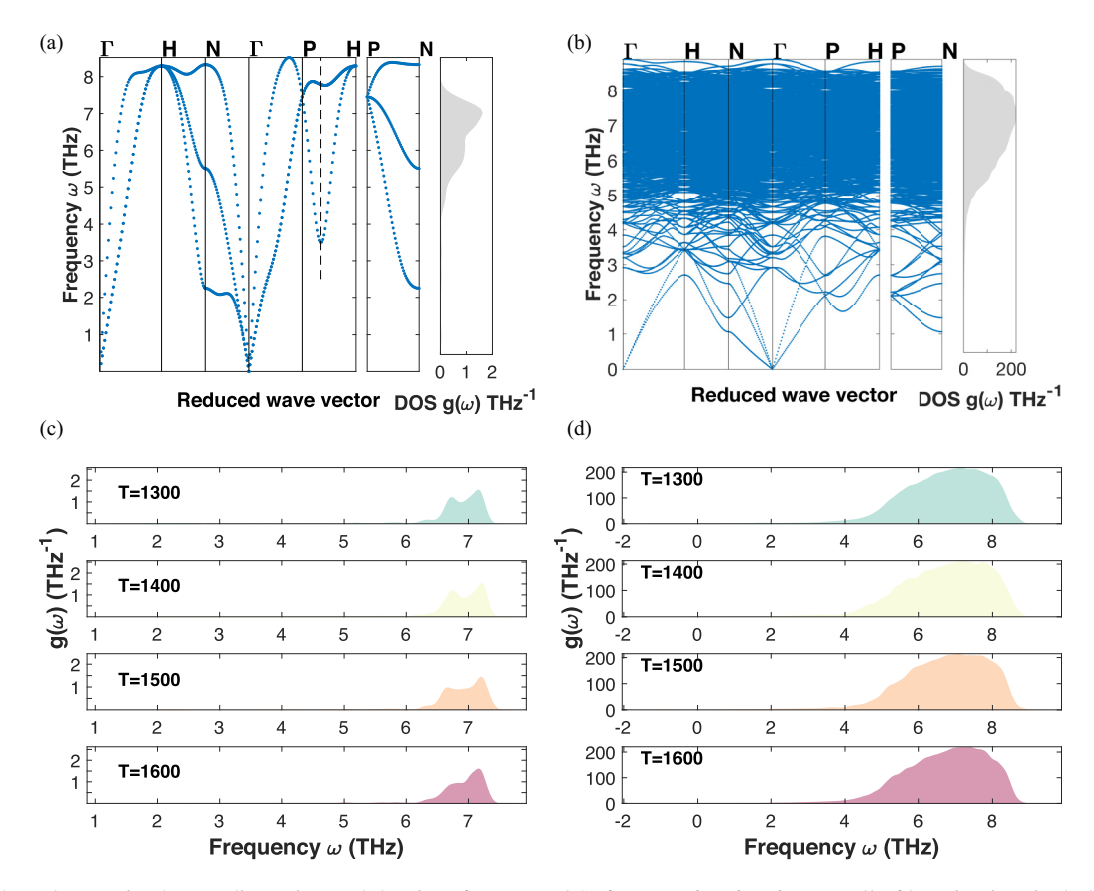


FIG. 3. The anharmonic phonon dispersion and density of states (DOS) for (a) a $6 \times 6 \times 6$ supercell of bcc titanium including 216 atoms and (b) bcc Ti with a monovacancy including 215 atoms at 1600 K. (c) The temperature-dependent DOS for bulk bcc Ti and (d) the bcc phase with a monovacancy at different temperatures.

effective potential (TDEP) method [63,64], to obtain the temperature-dependent phonon dispersion and DOS for well-defined equilibrium states, namely bulk bcc Ti and the bcc phase with a monovacancy (see Sec. SI in Ref. [51] for more details). Figure 2 compares the harmonic phonon dispersion (i.e., the zero-temperature phonon dispersion) of bcc Ti including phonon instabilities with finite-temperature phonon dispersions from 1300 K to 1600 K with no imaginary phonon frequencies, as expected due to dynamical stabilization of the phase (a similar plot for bcc Zr is presented in Fig. S6 in Ref. [51]).

As illustrated in Figs. 2(b)–2(d), there is a negative dip at $\xi=\frac{2}{3}$ on the $L\langle\xi\xi\xi\rangle$ phonon branch [depicted as the dashed line in Fig. 2(d)], which is indicative of the phonon softening effects. This phonon mode corresponds to the trigonal distortion in which two neighboring (111) planes move towards each other and results in the ω phase when they collapse [see Fig 2(e)]. This atomic distortion coincides with the vacancy jump direction for the bcc phase. Accordingly, we assume that the effective prefactor frequency, $\nu^*(T)$, which is the effective vibration frequency along the transition path, is equal to the temperature-dependent frequency of the $L_{\frac{2}{3}}\langle111\rangle$ phonon mode for the bulk bcc phase.

The successful jump frequency Γ can then be obtained given the anharmonic effective frequency ν^* and the activation free energy. To calculate the activation free energy in systems with harmonic phonon instabilities, there are some

bottlenecks. Since the structure is mechanically unstable and only stabilizes at high temperatures, it cannot be relaxed according to zero-temperature forces to obtain the vacancy formation enthalpy. Additionally, common schemes such as the nudged elastic band (NEB) or dimer method [65–67] cannot be used to locate the transition state as they rely on the assumption that the final and initial states of diffusion are metastable. Moreover, existence of imaginary phonon frequencies inhibits the calculation of vacancy formation entropy, S_{vib} . To overcome these problems, we use the statistical average energy and pressure from NVT ab initio molecular dynamics (AIMD) simulations to obtain the enthalpy of the system at high temperature. In addition, vacancy formation entropy is obtained by comparing the temperature-dependent phonon frequencies and DOS for the bulk and defected systems. For the specific problem of bcc IVB metals, we assume that an interpolated state between the initial and final states [see Fig. 1(d)] is a reasonable approximation for the transition state. Accordingly, all the parameters needed for diffusivity calculation in Eq. (1) can be obtained as temperaturedependent parameters that effectively account for phononphonon coupling effects:

$$D = \alpha a^{2} C_{v} \Gamma$$

$$= \alpha a^{2} v^{*}(T) \exp\left(\frac{-\Delta H_{m} - \Delta H_{v}(T)}{k_{B}T}\right) \exp\left(\frac{-\Delta S_{v}(T)}{k_{B}}\right).$$
(2)

III. APPLICATION TO THE BCC PHASE OF IVB METALS

We applied the proposed methodology to obtain the macroscopic diffusion coefficient for the bcc phase of titanium and zirconium. We calculate the migration enthalpy, ΔH_m , as the DFT energy difference between the intermediate state and the initial state [represented in Figs. 1(c) and 1(d)]. Note that we neglect the temperature-induced phonon-phonon coupling effects for the migration enthalpy calculation as the barrier energy for vacancy migration is calculated more accurately according to zero-temperature energies compared to the barrier energy for vacancy formation. This is because two more similar structures that both contain monovacancies are compared. Brute-force AIMD simulations cannot be used to calculate the enthalpy of the intermediate state since the simulation quickly slips away from this out-of-equilibrium state. A more sophisticated sampling technique is required which is the subject of a current development by the authors. The vacancy formation enthalpy is the difference of enthalpies for the bulk and defected systems and is obtained from ab initio molecular dynamics (AIMD) average energy and pressure (see Sec. SII in Ref. [51] for more details). Due to underestimation of DFT in obtaining the energy of the intrinsic surface formed around a vacancy, we add an explicit correction term to both the migration and vacancy formation enthalpies according to the electron density of the exchangecorrelation functional [68,69] (see Sec. SIII in Ref. [51] for more details). Figure 4(a) illustrates the vacancy formation enthalpy for bcc titanium above the allotropic transformation temperature (a similar plot is presented for bcc zirconium in Fig. S9(d) in Supplemental Material [51]).

Vacancy formation entropy is obtained by comparing the temperature-dependent phonon frequencies and DOS for the bulk and defected systems. Figures 3(a) and 3(b) illustrate the temperature-dependent phonon dispersion and DOS for both systems at 1600 K obtained using the TDEP method [63,64] (similar plots for bcc Zr are shown in Fig. S7 in Supplemental Material [51]). The formation of a vacancy results in the appearance of optical phonon branches by removing the periodicity of the crystal structure, and it broadens the peak in the DOS due to the existence of several localized modes at higher frequencies. The vibration entropy for the bulk and defected systems is obtained based on T-dependent phonon frequencies, $\omega(T)$, and DOS, $g(\omega(T))$ (see Sec. SIV in Supplemental Material [51]). Figures 3(c) and 3(d) show the anharmonic phonon density of states for both the bulk phase and the bcc phase including a monovacancy obtained by using the TDEP method at different temperatures (similar plots for bcc Zr are shown in Fig. S10 in Supplemental Material [51]). Creating a vacancy in the supercell results in a larger number of internal degrees of freedom, in this case $216 \times 3 - 3 = 645$, which is the area under the phonon density of states. The vacancy formation entropy for each temperature is shown in Fig. 4(b). As illustrated in Fig. 4(c), we calculate the equilibrium monovacancy concentration C_v , having the formation entropy ΔS_v and formation enthalpy ΔH_{ν} (see Sec. SIV in Supplemental Material [51]).

The *ab initio* predicted diffusivity for bcc titanium and zirconium alongside the parameters used in Eq. (2) are pre-

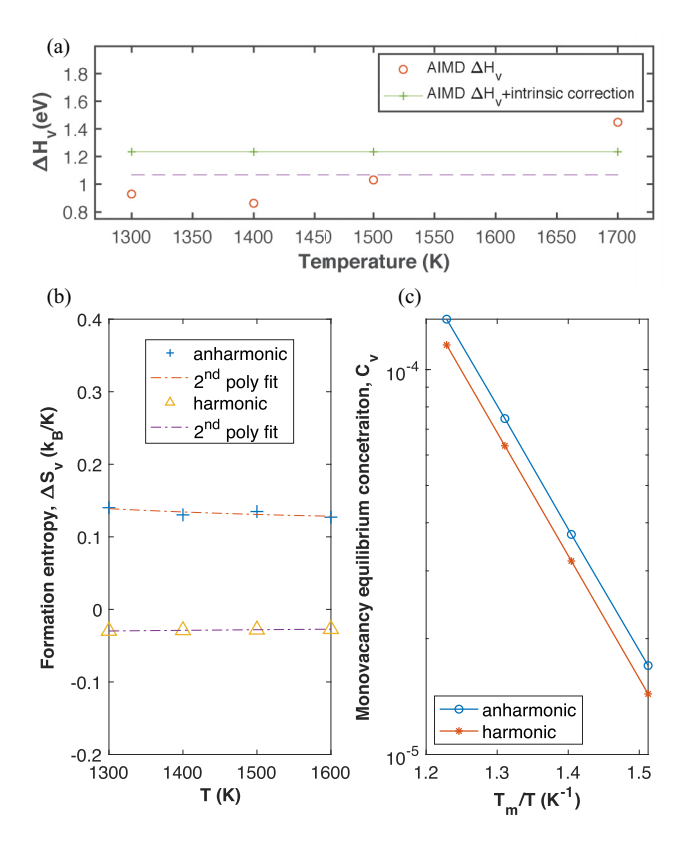


FIG. 4. (a) The vacancy formation enthalpy in bcc Ti as a function of temperature. The circles are the statistical average formation enthalpy obtained from AIMD simulation using the PBE exchange-correlation functional. The crosses are the formation enthalpy values including the explicit intrinsic surface correction term. (b) The formation entropy and (c) equilibrium vacancy concentration versus temperature for monovacancy in bcc Ti. For bulk bcc we used a $6\times6\times6$ supercell of bcc titanium including 216 atoms and for the defected system we used bcc Ti with a monovacancy including 215 atoms.

sented in Fig. 5. The circled curves in Fig. 5 are the diffusivity predictions by including the anharmonic lattice vibration effects, which agree well with experimental measurements of Ref. [40]. The diffusivity prediction based on the harmonic phonon analysis underestimates the diffusion coefficient by several orders of magnitude as shown by the crossed curves in Fig. 5. In spite of the fact that we use identical migration and formation enthalpies in both approaches, namely the proposed approach based on anharmonic phonon analysis and the standard harmonic model, the calculated diffusivities differ dramatically. Moreover, the vacancy formation entropy and concentration according to the proposed approach and the harmonic model are very similar for both bcc Ti and Zr (see Figs. 4(b) and 4(c) and Fig. S11 in Supplemental Material [51]). This further illustrates the significant role of anharmonic lattice vibrations in enhancing diffusivity in the bcc phase of Ti and Zr. The harmonic lattice vibration model underestimates the diffusivity by almost three orders of magnitude and two orders of magnitude for bcc Ti and bcc Zr, respectively (see next section for more details on harmonic model prediction).

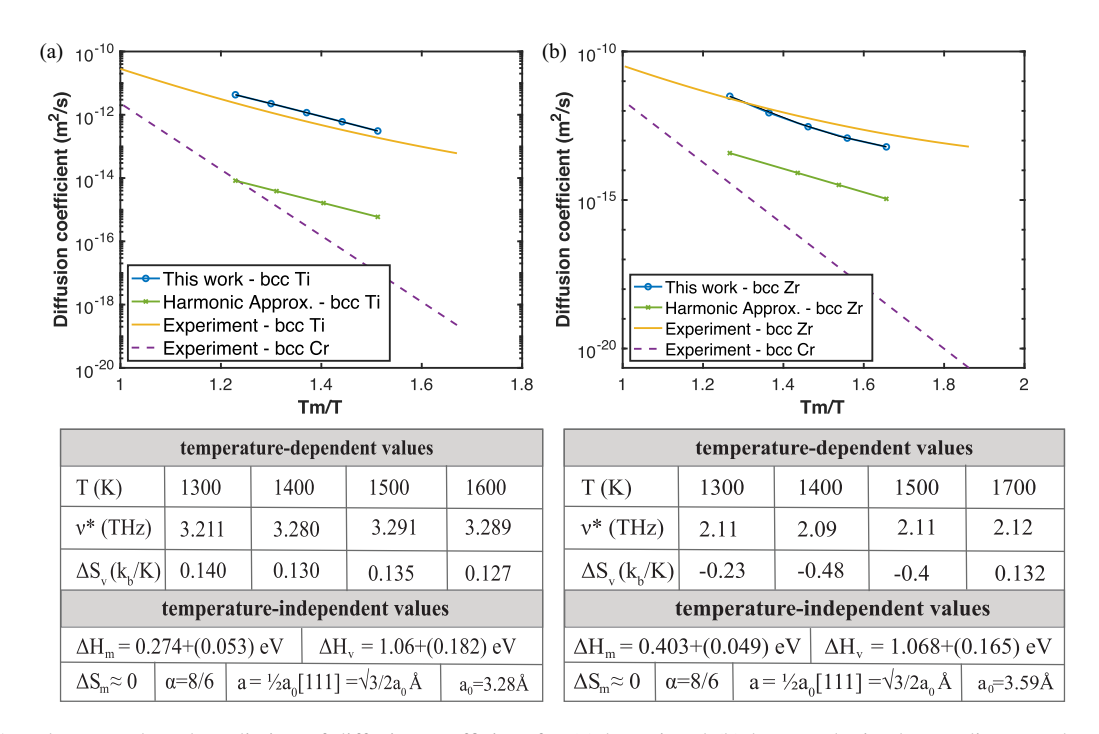


FIG. 5. Complete DFT-based prediction of diffusion coefficient for (a) bcc Ti and (b) bcc Zr obtained according to anharmonic phonon analysis (circled curves), validated with experimental measurements (solid curve) extracted from Ref. [40]. Diffusion coefficient for bcc Cr (dashed curve) is also extracted from Ref. [40] for comparison. Calculations based on standard harmonic phonon analysis (crosses) underestimate the diffusion coefficient by several orders of magnitude. T_m is equal to 1966 K and 2153 K for Ti and Zr, respectively. All the parameters for calculating the diffusion coefficient are presented in the tables. The internal surface correction terms for vacancy formation and migration enthalpies are presented in parentheses. v^* for each temperature is also represented by star marks in Fig. 2(d) for bcc Ti and Fig. S6 for bcc Zr.

IV. SIGNIFICANCE OF PHONON-PHONON COUPLING EFFECTS

To understand the significance of anharmonic vibration effects, we also calculated the diffusion coefficient according to a standard harmonic phonon analysis by excluding the imaginary harmonic phonon frequencies to calculate the vacancy formation entropy (see Sec. SIV in Ref. [51]). We also use the *T*-independent value $v_1 \times \frac{\prod_i v_i}{\prod_i v_i'}$ to obtain the v^* in Eq. (2) by assuming imaginary ν and ν' frequencies have real values. ν_1 is the most unstable phonon frequency (i.e., the square root of the most negative eigenvalue of the dynamical matrix) for the transition state. The transition state is assumed to be the estimated intermediate state presented in Fig. 1(d) for bcc Ti and in Fig. S5(d) for bcc Zr. We calculate v_1 to be 6.64 THz and 4.63 THz for Ti and Zr, respectively. This value is comparable to the temperature-dependent v^* in our approach, presented in Fig. 5. However, the effective jump prefactor v^* is severely low in the harmonic approximation. This is due to the small value for $\frac{\prod_i v_i}{\prod_i v_i}$, which essentially assumes phonon modes are independent (decoupled) oscillators and neglect phonon-phonon coupling effects. This assumption is severely underperforming for calculating the diffusion coefficient in phases with harmonic phonon instabilities, not simply due to infeasibility of its application but more importantly because of the dominant effect of anharmonic phonon interactions. We calculate the ratio of the product of independent harmonic phonon frequencies in the initial and intermediate states, $\frac{\prod_i v_i}{\prod_i v_i'}$

to be 0.0011 and 0.0073 for bcc Ti and Zr, respectively, which results in ν^* values of 0.0073 THz and 0.034 THz for bcc Ti and Zr, respectively. Typical ratio values of $\frac{\prod_i \nu_i}{\prod_i \nu_i'}$ for solid phases that are mechanically stable and can be accurately described by harmonic phonon modes are orders of magnitude higher. For example, the ratio value for fcc Al is 5.6 and for fcc Ag is 6.94. We obtained these values by comparing the DFT harmonic phonon eigenvalues for the initial and saddle point configuration obtained from the nudged elastic band method and they are reported in our previous work [50].

V. COMPUTATIONAL DETAILS

A. DFT calculation

Electronic structure calculations are performed using density functional theory (DFT) as implemented in the Vienna *ab initio* simulation package (VASP) [70–73]. We use the projector augmented wave (PAW) method [73,74] with energy cutoff of 274.6 eV for Ti and 229.9 eV for Zr and the generalized gradient approximation (GGA) [72,73,75] with the PBE [76] exchange correlation (Ti_pv and Zr_sv). All DFT calculations, including static energy, molecular dynamics, and SCAILD are performed on a $6 \times 6 \times 6$ supercell of bcc including 216 atoms and a supercell with a vacancy at the bcc site. For bcc Cr, we use the energy cutoff of 395.5 eV for the PAW pseudopotential with the PBE [76] exchange-correlation functional for a supercell of 128 atoms for the bulk phase and 127 atoms for the bcc phase with a monovacancy.

B. Enthalpy calculations

AIMD simulations are performed at constant volume and temperature (NVT) under the Nose-Hoover thermostat [77–81]. Enthalpy values for the bulk and defected systems are obtained by averaging AIMD kinetic and potential energies and the pressure-volume term that are captured every 0.1 ps for a 35 ps trajectory after 1 ps thermalization at each temperature (see Sec. SII in Ref. [51] for more details).

C. Phonon analysis

SCAILD iteratively converges the phonon frequencies at different temperatures accounting for anharmonic effects [60-62]. In TDEP, the temperature-dependent forceconstant tensor is obtained by minimizing the difference between ab initio molecular dynamics (AIMD) forces and forces described in the harmonic approximation [63,64] (see Sec. SI in Ref. [51] for details). SCAILD method is performed using the SCPH code [61] based on DFT calculations until the free energy difference converges to 10^{-5} eV (see Sec. SI in Ref. [51]). For the DFT calculations the Brillouin zone integration is performed on a mesh density of 4000 points per reciprocal angstrom (generated by the EZVASP module [82]). In TDEP method, phonon dispersions and DOSs are obtained from temperature-dependent force constant tensors using the PHONOPY code [83]. The temperature-dependent force constant tensor is obtained by least square fitting of AIMD forces and displacements to a harmonic model using our in-house code. For AIMD simulations, the first Brillouin zone integration is performed on the Γ point for a 6 \times 6 \times 6 supercell of bcc with cell volume of 3799.45 Å³ and 4988.63 Å³ for Ti and Zr, respectively.

VI. DISCUSSION

The agreement of our first-principles prediction with experimental diffusion coefficient indicates that monovacancy jumps are the dominant atomic mechanism responsible for macroscopic diffusion in the bcc phase of IIIB-IVB metals. The anomalously larger diffusivity in bcc IIIB-IVB metals compared to other bcc and fcc metals can be accurately accounted for by including temperature-dependent anharmonic lattice vibration effects within the transition state theory to describe monovacancy jumps. In other words, monovacancy jumps are significantly promoted due to phonon-phonon coupling effects in these phases. On the other hand, the nature of free energy surface in bcc IIIB-IVB metals, which consists of multiple local minima around the bcc structure, results in hopping of the system among local structural distortions (this has been shown for bcc Ti and B2 NiTi in our previous studies [22,28]) and increases the likelihood of collective atomic motion. This phenomenon has been observed as heterophase fluctuations in earlier works [41,84] and as a concerted stringlike atomic motion in a more recent ab initio molecular dynamics simulation [44]. However, our calculations show that these collective motions do not contribute to the macroscopic diffusivity, in other words they do not result in a long range mass transport. The contribution of collective atomic motion to diffusivity can be the subject of a future investigation which requires long-time molecular dynamics simulation (which is feasible based on potential models) for a complete statistical sampling of the diffusion process (similar to methods used to distinguish cyclic collective motion in tetragonal Li7La3Zr2O12 (LLZO) [85]). One possibility is that these collective atomic motions are cyclic or have a random nature with a zero long-range effect. Unfortunately, the current potential models for bcc Ti (e.g., the MEAM potential [86]) cannot effectively capture the softening of the $L_3^2(111)$ phonon, which plays the major role in softening of restoring forces and collective atomic distortions. The phonon-assisted vacancy jump mechanism to be the predominant one in bcc IVB metals is supported by direct experimental determination of the mechanism [31–33,35] and the isotope effect [46,47].

While self-consistent harmonic approximation (SCHA) approaches (e.g., SCAILD and TDEP) have been extensively used for thermodynamic description of various systems [61-64,87-90], we utilize self-consistent temperaturedependent phonon analysis to describe diffusive jump rates within the framework of the transition state theory. The introduced approach can be used for diffusion description of other mechanically unstable phases, including the β phase of IIIB and IVB metals and their alloys. The computation cost of the introduced methodology is minimal, only requiring anharmonic phonon analysis of two systems (a bulk phase and a small supercell including a vacancy) at each temperature, when compared to diffusion description based on brute-force molecular dynamic simulation on the order of nanoseconds (refer to Ref. [85] for details on adequate MD sampling of diffusive events).

Developing a general framework that effectively accounts for temperature-induced effects in diffusion description of mechanically unstable but dynamically stabilized phases is beyond the scope of this report and is the subject of an active investigation by the authors. The major assumption in calculation of diffusivity in this report is the approximation of migration energy barrier and the effective jump frequency along the migration path (details are described in Sec. III). These assumptions are justified for the pure bcc phase due to the coincidence of diffusive jump direction and a specific phonon mode with softening effects.

In summary, we predict the diffusivity of the bcc Ti and Zr by simply including temperature-induced anharmonic phonon-phonon coupling effects within the monovacancy-mediated diffusive jump process. Our predictions are in good agreement with experimental measurements while disregarding the anharmonic vibration effects results in orders of magnitude underestimation in diffusivity. Our findings shed light on the underlying mechanism responsible for markedly larger diffusion coefficient in bcc IIIB and IVB metals and provide a computationally efficient and accurate approach for macroscopic diffusivity calculations beyond the harmonic lattice vibration approximation.

ACKNOWLEDGMENTS

We would like to thank Dr. John W. Lawson and Dr. Justin Haskins from NASA Ames Research Center for kindly sharing their code for *T*-dependent force-constant tensor calculation. Our in-house code is a modification of their code. This work is supported by Dr. Kadkhodaei's startup funding

at the University of Illinois at Chicago. Some of the calculations in this work were performed on the Extreme Science

and Engineering Discovery Environment (XSEDE) resource through allocation TG-DMR190017 [91].

- M. Mantina, Y. Wang, R. Arroyave, L. Q. Chen, Z. K. Liu, and C. Wolverton, First-Principles Calculation of Self-Diffusion Coefficients, Phys. Rev. Lett. 100, 215901 (2008).
- [2] M. Mantina, Y. Wang, L. Q. Chen, Z. K. Liu, and C. Wolverton, First principles impurity diffusion coefficients, Acta Mater. 57, 4102 (2009).
- [3] H. H. Wu and D. R. Trinkle, Direct Diffusion through Interpenetrating Networks: Oxygen in Titanium, Phys. Rev. Lett. 107, 045504 (2011).
- [4] E. Wimmer, W. Wolf, Jürgen Sticht, P. Saxe, Clint B. Geller, R. Najafabadi, and George A. Young, Temperature-dependent diffusion coefficients from ab initio computations: Hydrogen, deuterium, and tritium in nickel, Phys. Rev. B 77, 134305 (2008).
- [5] Marina V. Koudriachova, Nicholas M. Harrison, and Simon W. de Leeuw, Diffusion of Li-ions in rutile. An ab initio study, Solid State Ionics 157, 35 (2003).
- [6] C. Domain and C. S. Becquart, Diffusion of phosphorus in α -Fe: An ab initio study, Phys. Rev. B **71**, 214109 (2005).
- [7] J. D. Tucker, R. Najafabadi, T. R. Allen, and D. Morgan, Ab initio-based diffusion theory and tracer diffusion in Ni–Cr and Ni–Fe alloys, J. Nucl. Mater. 405, 216 (2010).
- [8] J. Sarnthein, K. Schwarz, and P. E. Blöchl, Ab initio moleculardynamics study of diffusion and defects in solid Li₃N, Phys. Rev. B 53, 9084 (1996).
- [9] S. Choudhury, L. Barnard, J. D. Tucker, T. R. Allen, B. D. Wirth, M. Asta, and D. Morgan, Ab-initio based modeling of diffusion in dilute bcc Fe–Ni and Fe–Cr alloys and implications for radiation induced segregation, J. Nucl. Mater. 411, 1 (2011).
- [10] Peter E. Blöchl, C. G. Van de Walle, and S. T. Pantelides, First-Principles Calculations of Diffusion Coefficients: Hydrogen in Silicon, Phys. Rev. Lett. 64, 1401 (1990).
- [11] A. Van der Ven, John C. Thomas, Q. Xu, B. Swoboda, and D. Morgan, Nondilute diffusion from first principles: Li diffusion in Li_xTiS₂, Phys. Rev. B 78, 104306 (2008).
- [12] A. Van der Ven, G. Ceder, M. Asta, and P. D. Tepesch, First-principles theory of ionic diffusion with nondilute carriers, Phys. Rev. B **64**, 184307 (2001).
- [13] Mikhail I. Mendelev and Y. Mishin, Molecular dynamics study of self-diffusion in bcc Fe, Phys. Rev. B 80, 144111 (2009).
- [14] V. Milman, M. C. Payne, V. Heine, R. J. Needs, J. S. Lin, and M. H. Lee, Free Energy and Entropy of Diffusion by ab initio Molecular Dynamics: Alkali Ions in Silicon, Phys. Rev. Lett. 70, 2928 (1993).
- [15] W. Frank, U. Breier, C. Elsässer, and M. Fähnle, First-Principles Calculations of Absolute Concentrations and Self-Diffusion Constants of Vacancies in Lithium, Phys. Rev. Lett. 77, 518 (1996).
- [16] H. Eyring, The activated complex in chemical reactions, J. Chem. Phys. 3, 107 (1935).
- [17] George H. Vineyard, Frequency factors and isotope effects in solid state rate processes, J. Phys. Chem. Solids 3, 121 (1957).

- [18] Göran Grimvall, B. Magyari-Köpe, V. Ozolinš, and Kristin A. Persson, Lattice instabilities in metallic elements, Rev. Mod. Phys. 84, 945 (2012).
- [19] K. Einarsdotter, B. Sadigh, G. Grimvall, and V. Ozolinš, Phonon Instabilities in fcc and bcc Tungsten, Phys. Rev. Lett. 79, 2073 (1997).
- [20] A. P. Mirgorodsky, M. B. Smirnov, and P. E. Quintard, Latticedynamical study of the cubic-tetragonal-monoclinic transformations of zirconia, Phys. Rev. B 55, 19 (1997).
- [21] K. Parlinski, Z. Q. Li, and Y. Kawazoe, First-Principles Determination of the Soft Mode in Cubic ZrO 2, Phys. Rev. Lett. 78, 4063 (1997).
- [22] S. Kadkhodaei, Qi-Jun Hong, and A. van de Walle, Free energy calculation of mechanically unstable but dynamically stabilized bcc titanium, Phys. Rev. B 95, 064101 (2017).
- [23] K. Persson, M. Ekman, and V. Ozolinš, Phonon instabilities in bcc Sc, Ti, La, and Hf, Phys. Rev. B **61**, 11221 (2000).
- [24] P. J. Craievich, J. M. Sanchez, R. E. Watson, and M. Weinert, Structural instabilities of excited phases, Phys. Rev. B 55, 787 (1997).
- [25] Y. Y. Ye, Y. Chen, K. M. Ho, B. N. Harmon, and P. A. Lindgard, Phonon-Phonon Coupling and the Stability of the High-Temperature Bcc Phase of Zr, Phys. Rev. Lett. 58, 1769 (1987).
- [26] Q. Xu and A. Van der Ven, First-principles investigation of metal-hydride phase stability: The Ti-H system, Phys. Rev. B 76, 064207 (2007).
- [27] R. Quijano, R. de Coss, and David J. Singh, Electronic structure and energetics of the tetragonal distortion for TiH 2, ZrH 2, and HfH 2: A first-principles study, Phys. Rev. B 80, 184103 (2009)
- [28] S. Kadkhodaei and A. van de Walle, First-principles calculations of thermal properties of the mechanically unstable phases of the PtTi and NiTi shape memory alloys, Acta Mater. 147, 296 (2018).
- [29] A. T. Zayak, P. Entel, J. Enkovaara, A. Ayuela, and R. M. Nieminen, First-principles investigation of phonon softenings and lattice instabilities in the shape-memory system Ni 2 MnGa, Phys. Rev. B 68, 132402 (2003).
- [30] G. Vogl, W. Miekeley, A. Heidemann, and W. Petry, Anomalously Fast Diffusion of Cobalt in β-Zirconium: Evidence for Two Different Jump Frequencies from Quasielastic Neutron Scattering, Phys. Rev. Lett. 53, 934 (1984).
- [31] G. Vogl, W. Petry, Th. Flottmann, and A. Heiming, Direct determination of the self-diffusion mechanism in bcc-titanium, Phys. Rev. B **39**, 5025 (1989).
- [32] R. F. Peart and D. H. Tomlin, Diffusion of solute elements in beta-titanium, Acta Metall. 10, 123 (1962).
- [33] W. Petry, A. Heiming, J. Trampenau, and G. Vogl, On the Diffusion Mechanism in the bcc Phase of the Group 4 Metals, in *Diffusion in Metals and Alloys*, Defect and Diffusion Forum (Trans Tech Publications, Switzerland, 1991), Vol. 66, pp. 157–174.

- [34] C. Herzig, J. Neuhaus, K. Vieregge, and L. Manke, Fast impurity diffusion of Co and Fe in β-Zr and β-Zr-alloys, in *Vacancies and Interstitials in Metals and Alloys*, Materials Science Forum (Trans Tech Publications, Switzerland, 1987), Vol. 15, pp. 481–486.
- [35] W. Petry, T. Flottmann, A. Heiming, J. Trampenau, M. Alba, and G. Vogl, Atomistic Study of Anomalous Self-Diffusion in Bcc β-Titanium, Phys. Rev. Lett. 61, 722 (1988).
- [36] C. Herzig, U. Köhler, and S. V. Divinski, Tracer diffusion and mechanism of non-Arrhenius diffusion behavior of Zr and Nb in body-centered cubic Zr–Nb alloys, J. Appl. Phys. 85, 8119 (1999).
- [37] H. M. Gilder and D. Lazarus, Role of vacancy anharmonicity on non-Arrhenius diffusional behavior, Phys. Rev. B 11, 4916 (1975).
- [38] J. M. Sanchez and D. De Fontaine, Model for Anomalous Self-Diffusion in Group-IVB Transition Metals, Phys. Rev. Lett. 35, 227 (1975).
- [39] J. M. Sanchez and D. De Fontaine, Anomalous diffusion in omega forming systems, Acta Metall. 26, 1083 (1978).
- [40] C. Herzig and U. Köhler, Anomalous self-diffusion in BCC IVB metals and alloys, Mater. Sci. Forum 15–18, 301 (1987).
- [41] G. Vogl, Fast solute diffusion in metals and the tendency for heterophase fluctuations, Europhys. Lett. 13, 149 (1990).
- [42] C. Herzig, The correlation between diffusion behavior and phonon softening in bcc metals, Ber. Bunsen Ges. Phys. Chem. 93, 1247 (1989).
- [43] S. L. Dudarev, The non-arrhenius migration of interstitial defects in bcc transition metals, C. R. Phys. 9, 409 (2008).
- [44] D. G. Sangiovanni, J. Klarbring, D. Smirnova, N. V. Skripnyak, D. Gambino, M. Mrovec, S. I. Simak, and I. A. Abrikosov, Superioniclike Diffusion in an Elemental Crystal: Bcc Titanium, Phys. Rev. Lett. 123, 105501 (2019).
- [45] M. I. Mendelev and B. S. Bokstein, Molecular dynamics study of self-diffusion in zr, Philos. Mag. 90, 637 (2010).
- [46] L. Manke and C. Herzig, Diffusion und isotopieeffekt von silber in β -Zirkon, Acta Metall. **30**, 2085 (1982).
- [47] M. S. Jackson and D. Lazarus, Isotope effect for diffusion of tin in *β*-titanium, Phys. Rev. B **15**, 4644 (1977).
- [48] P. Shewmon, *Diffusion in Solids* (Springer International Publishing, Basel, Switzerland, 2016).
- [49] H. Mehrer, Diffusion in Solids: Fundamentals, Methods, Materials, Diffusion-Controlled Processes (Springer, Berlin, Heidelberg, 2007).
- [50] S. Kadkhodaei and A. van de Walle, A simple local expression for the prefactor in transition state theory, J. Chem. Phys. **150**, 144105 (2019).
- [51] See Supplemental Material at http://link.aps.org/supplemental/ 10.1103/PhysRevMaterials.4.043802 for details on calculation of anharmonic phonon dispersion and density of states, vacancy formation enthalpy, vacancy internal surface energy correction term, vacancy formation entropy and equilibrium concentration, and details for diffusivity calculation in bcc zirconium [92–96].
- [52] S. Kadkhodaei and A. van de Walle, Software tools for thermodynamic calculation of mechanically unstable phases from first-principles data, Comput. Phys. Commun. **246**, 106712 (2020).
- [53] V. Ozolins, First-Principles Calculations of Free Energies of Unstable Phases: The Case of fcc W, Phys. Rev. Lett. 102, 065702 (2009).

- [54] J. C. Thomas and A. Van der Ven, Elastic properties and stresstemperature phase diagrams of high-temperature phases with low-temperature lattice instabilities, Phys. Rev. B 90, 224105 (2014).
- [55] R. G. Hennig, T. J. Lenosky, D. R. Trinkle, S. P. Rudin, and J. W. Wilkins, Classical potential describes martensitic phase transformations between the α , β , and ω titanium phases, Phys. Rev. B **78**, 054121 (2008).
- [56] Z.-G. Mei, S.-L. Shang, Y. Wang, and Z.-K. Liu, Density-functional study of the thermodynamic properties and the pressure–temperature phase diagram of Ti, Phys. Rev. B 80, 104116 (2009).
- [57] F. Zhou, W. Nielson, Y. Xia, and V. Ozolinš, Lattice Anharmonicity and Thermal Conductivity from Compressive Sensing of First-Principles Calculations, Phys. Rev. Lett. 113, 185501 (2014).
- [58] A. I. Duff, T. Davey, D. Korbmacher, A. Glensk, B. Grabowski, J. Neugebauer, and M. W. Finnis, Improved method of calculating ab initio high-temperature thermodynamic properties with application to ZrC, Phys. Rev. B 91, 214311 (2015).
- [59] J. Z. Liu, A. van de Walle, G. Ghosh, and M. Asta, Structure, energetics, and mechanical stability of fe-cu bcc alloys from first-principles calculations, Phys. Rev. B **72**, 144109 (2005).
- [60] N. R. Werthamer, Self-Consistent Phonon Formulation of Anharmonic Lattice Dynamics, Phys. Rev. B 1, 572 (1970).
- [61] P. Souvatzis, O. Eriksson, M. I. Katsnelson, and S. P. Rudin, Entropy Driven Stabilization of Energetically Unstable Crystal Structures Explained from First Principles Theory, Phys. Rev. Lett. 100, 095901 (2008).
- [62] P. Souvatzis, O. Eriksson, M. I. Katsnelson, and S. P. Rudin, The self-consistent ab initio lattice dynamical method, Comput. Mater. Sci. 44, 888 (2009).
- [63] O. Hellman, I. A. Abrikosov, and S. I. Simak, Lattice dynamics of anharmonic solids from first principles, Phys. Rev. B 84, 180301(R) (2011).
- [64] O. Hellman, P. Steneteg, I. A. Abrikosov, and S. I. Simak, Temperature dependent effective potential method for accurate free energy calculations of solids, Phys. Rev. B 87, 104111 (2013).
- [65] G. Henkelman and H. Jónsson, Improved tangent estimate in the nudged elastic band method for finding minimum energy paths and saddle points, J. Chem. Phys. 113, 9978 (2000).
- [66] G. Henkelman, B. P. Uberuaga, and H. Jónsson, A climbing image nudged elastic band method for finding saddle points and minimum energy paths, J. Chem. Phys. 113, 9901 (2000).
- [67] G. Henkelman and H. Jónsson, A dimer method for finding saddle points on high dimensional potential surfaces using only first derivatives, J. Chem. Phys. 111, 7010 (1999).
- [68] K. Carling, G. Wahnström, T. R. Mattsson, A. E. Mattsson, N. Sandberg, and G. Grimvall, Vacancies in Metals: From First-Principles Calculations to Experimental Data, Phys. Rev. Lett. 85, 3862 (2000).
- [69] T. R. Mattsson and A. E. Mattsson, Calculating the vacancy formation energy in metals: Pt, pd, and mo, Phys. Rev. B 66, 214110 (2002).
- [70] G. Kresse and J. Hafner, Ab initio molecular dynamics for liquid metals, Phys. Rev. B 47, 558 (1993).
- [71] G. Kresse and J. Furthmüller, Efficiency of ab-initio total energy calculations for metals and semiconductors using a planewave basis set, Comput. Mater. Sci. 6, 15 (1996).

- [72] G. Kresse and J. Furthmüller, Efficient iterative schemes for ab initio total-energy calculations using a plane-wave basis set, Phys. Rev. B **54**, 11169 (1996).
- [73] G. Kresse and D. Joubert, From ultrasoft pseudopotentials to the projector augmented-wave method, Phys. Rev. B **59**, 1758 (1999).
- [74] P. E. Blöchl, Projector augmented-wave method, Phys. Rev. B 50, 17953 (1994).
- [75] J. P. Perdew, Generalized gradient approximation for the fermion kinetic energy as a functional of the density, Phys. Lett. A 165, 79 (1992).
- [76] J. P. Perdew, K. Burke, and M. Ernzerhof, Generalized Gradient Approximation Made Simple. Phys. Rev. Lett. 77, 3865 (1996).
- [77] W. G. Hoover and B. L. Holian, Kinetic moments method for the canonical ensemble distribution, Phys. Lett. A 211, 253 (1996).
- [78] S. Nosé, A molecular dynamics method for simulations in the canonical ensemble, Mol. Phys. 52, 255 (1984).
- [79] S. Nosé, A unified formulation of the constant temperature molecular dynamics methods, J. Chem. Phys. 81, 511 (1984).
- [80] W. G. Hoover, Canonical dynamics: Equilibrium phase-space distributions, Phys. Rev. A 31, 1695 (1985).
- [81] G. J. Martyna, M. L. Klein, and M. Tuckerman, Nosé-Hoover chains: The canonical ensemble via continuous dynamics, J. Chem. Phys. 97, 2635 (1992).
- [82] A. van de Walle and G. Ceder, Automating first-principles phase diagram calculations, J. Phase Equilib. 23, 348 (2002).
- [83] A. Togo and I. Tanaka, First principles phonon calculations in materials science, Scr. Mater. 108, 1 (2015).
- [84] A. Heiming, W. Petry, J. Trampenau, M. Alba, C. Herzig, and G. Vogl, Phonons and martensitic phase transitions in pure bcc Ti and bcc Zr, Phys. Rev. B 40, 11425 (1989).
- [85] M. Burbano, D. Carlier, F. Boucher, B. J. Morgan, and M. Salanne, Sparse Cyclic Excitations Explain the Low Ionic Conductivity of Stoichiometric li₇la₃zr₂o₁₂, Phys. Rev. Lett. 116, 135901 (2016).
- [86] W.-S. Ko, B. Grabowski, and J. Neugebauer, Development and application of a Ni-Ti interatomic potential with high predictive

- accuracy of the martensitic phase transition, Phys. Rev. B 92, 134107 (2015).
- [87] A. van Roekeghem, J. Carrete, and N. Mingo, Anomalous thermal conductivity and suppression of negative thermal expansion in ScF₃, Phys. Rev. B **94**, 020303(R) (2016).
- [88] I. Errea, M. Calandra, and F. Mauri, Anharmonic free energies and phonon dispersions from the stochastic self-consistent harmonic approximation: Application to platinum and palladium hydrides, Phys. Rev. B 89, 064302 (2014).
- [89] R. Bianco, I. Errea, L. Paulatto, M. Calandra, and F. Mauri, Second-order structural phase transitions, free energy curvature, and temperature-dependent anharmonic phonons in the self-consistent harmonic approximation: Theory and stochastic implementation, Phys. Rev. B 96, 014111 (2017).
- [90] P. Korotaev, M. Belov, and A. Yanilkin, Reproducibility of vibrational free energy by different methods, Comput. Mater. Sci. 150, 47 (2018).
- [91] J. Towns, T. Cockerill, M. Dahan, I. Foster, K. Gaither, A. Grimshaw, V. Hazlewood, S. Lathrop, D. Lifka, G. D. Peterson, R. Roskies, J. R. Scott, and N. Wilkins-Diehr, Xsede: Accelerating scientific discovery, Comput. Sci. Eng. 16, 62 (2014).
- [92] Appendix d statistical errors, in *Understanding Molecular Simulation (2nd ed.)*, edited by D. Frenkel and B. Smit (Academic Press, San Diego, 2002), p. 525.
- [93] C. Freysoldt, B. Grabowski, T. Hickel, J. Neugebauer, G. Kresse, A. Janotti, and C. G. Van de Walle, First-principles calculations for point defects in solids, Rev. Mod. Phys. 86, 253 (2014).
- [94] R. Nazarov, T. Hickel, and J. Neugebauer, Vacancy formation energies in fcc metals: Influence of exchange-correlation functionals and correction schemes, Phys. Rev. B 85, 144118 (2012).
- [95] A. E. Mattsson, R. R. Wixom, and R. Armiento, Electronic surface error in the si interstitial formation energy, Phys. Rev. B 77, 155211 (2008).
- [96] A. E. Mattsson, R. Armiento, P. A. Schultz, and T. R. Mattsson, Nonequivalence of the generalized gradient approximations pbe and pw91, Phys. Rev. B 73, 195123 (2006).